

pGenesis Multicompartment Computational Model Detailed Description (Kudela, Anderson)

Cortical network

The spatial arrangement of neurons is based on our previous implementations of single compartment neurons arranged around a minicolumnar square lattice format (1). The modeled cortical volume was divided into a three layers as shown in **Fig 2**: supragranular (basket, pyramidal, low threshold spiking and axo-axonic neurons in layers II/III), internal granular layer (stellate neurons in layer IV) and infragranular (basket, low threshold spiking and axo-axonic in layer V and pyramidal neurons in layers V and VI). The position of a neuron within a simulated volume is defined by the Cartesian coordinates of the soma. Coordinates of the proximal and distal compartments are calculated relative to the position of the soma. The vertical location of a neuron within a minicolumn is random within a given range that is pre-determined for each cell type and each neuron is rotated about its normal axis by a random angle from 0 to 360 degrees. This allows for the vertical arrangement of neuron types into a layered structure within a simulated volume similar to that found in corresponding cortical layers. The exceptions are thalamic cells which were not vertically arranged but held at a fixed depth below the simulated layers (2).

In the horizontal direction we use an array of repeating minicolumns (3,4) to create the modeled cortical volume. The arrangement of neurons in layers and minicolumns provides a spatial scale in both vertical and horizontal directions. An array of 40x40 repeating minicolumns represents approximately 1 mm x 1 mm of cortex. The cellular density in the model varies from 630 (basket) to 5043 (pyramidal) neurons/mm³. The typical cortical volume used in the simulation has a size of 2.4 mm × 2.4 mm × 3.2 mm, and consists of a 96 × 96 array of repeating minicolumnar local circuits. Both the vertical and the horizontal size for the modeled volume are chosen as an approximate representation of human cortex, with a total simulated thickness (above the white matter) of 3195 μm (5,6) and 25 μm interspacing between cortical minicolumns (3,4). The centers of the cortical layers were taken at z-positions 2938 μm (layer I), 2614 μm (layer II), 1980 μm (III), 1337 μm (IV), 656 μm (V), 280 μm (VI) above the white matter. Relative positions of the cells (with the exception of thalamic cells) are demonstrated in **Fig 2**. The cellular density in the model ranges from 630 (basket) to 5043 (pyramidal) neurons/mm³.

The minicolumns are composed of excitatory cells including: 4 Layer II/III regular spiking (RS) pyramidal cells, one Layer IV RS stellate cell, 4 each of Layer V intrinsic bursting (IB) and VI RS pyramidal cells, one Layer V RS pyramidal cell, and in every fourth minicolumn one Layer II/III fast rhythmic bursting (FRB) pyramidal cell. Inhibitory cells include one of each alternating in successive minicolumns: supra- and infragranular fast spiking (FS) basket, supra- and infragranular low threshold spiking (LTS), and supra- and infragranular FS axo-axonic cells. The minicolumns containing infragranular inhibitory cells are also wired to one thalamocortical relay cell (TCR) and one inhibitory thalamic reticular nucleus cell (nRT) to complete the thalamocortical connectivity.

The multicompartment models of the rendered cells are shown in Figures 1A-F. Each neuron has a single compartment soma, a 6-compartment branching axon, and multiple dendritic compartments. The Layer II/III is composed of RS (74 compartments) and FRB (74 compartments) pyramidal cell subtypes. The Layer IV consists of RS stellate cells (59 compartments). Layers V and VI have pyramidal cells, with the Layer V cells consisting of the IB (61 compartments) and RS (74 compartments) subtypes, and the Layer VI cells being RS (50 compartments). There are also superficial and deep representations of the basket (59 compartments, modeled as FS cell type), LTS (59 compartments, RS type), and axo-axonic (59 compartments, FS type) cells. The TCR have 137 compartments and the nRT cells have 59 compartments. These neuron models were used previously to study high frequency gamma oscillations, sleep spindles and epileptogenic bursts (7) and the cellular electrophysiology parameters follow closely those of (7-9). The conductance densities of various compartmental regions for modeled neurons are listed in Table 1. The modifications that have been made in these models include solely neuronal structural differences such as: 1) dendritic/axonal 3D representations along the neuron's normal axis and 2) axons directed perpendicular to the pia rather than the tangential plane. Taking into the account the 3D spatial structure of neurons allows replicate details of the dendritic morphologies of modeled neurons in the modeled cortex. Neuronal model 3D structures and their compartmental representations have been implemented in the GENESIS 2.3 simulation platform.

Network Connectivity

Intracellular communication includes chemical synapses (AMPA, NMDA, and GABA_A receptors) as well as gap junctions implemented in the Genesis environment (10-11). Synaptic connections are modeled with the help of GENESIS synchan objects, with specific synaptic current rise/decay times fitted to either single (AMPA, GABA_A) or dual (NMDA) exponential functions based on their presynaptic cell type. The active cable effects of postsynaptic transmission are approximated by the multicompartmental structure and embedded channel dynamics of the postsynaptic cells. The patterns of synaptic connections on the postsynaptic dendritic trees are patterned closely after (7). The synapses on the various represented compartments follow the conductances and time-scales of (7) closely and typically range from 0.01 nS to 2 nS. The parameters of the synaptic conductance functions used in the simulations are provided in Table 2. Gap junctions occur between Layer II/III pyramidal cells, Layer V pyramidal cells, supra- and infra-granular basket cells taken separately, Layer VI pyramidal cells, stellate cells, supra- and infra-granular LTS cells taken separately, and reticular nucleus cells. Gap junction connection probabilities and gap junction conductances are provided in Table 3.

The connectivity pattern (wiring) is similar, and includes local random connectivity as in (7) with most connections extending maximally to the approximate size of a cortical macrocolumn (250-300 μm). A table of connection probabilities with maximum connection ranges is provided (Table 4 & 5). Wiring intrinsic and external to the minicolumns is guided by the neocortical models of Douglas and Martin (12), as well as the more general cortical connectivity provided by Nieuwenhuys (13). Data for both the short range (<50-200 μm) and longer range inhibitory connections is obtained from several histological studies (14-19). These specify parameters for the area of local isotropic connectivity, the rate of decay of connections in the decreasing zone of connectivity, and the numbers of excitatory and inhibitory neurons contacted. The long range connection data of the pyramidal cells, specifically the lateral connectivity of the Layer II/III, and Layer V pyramidal cells out to 1-2 mm is also drawn from histology sources (20-22).

The basic connectivity pattern was drawn from a variety of cortical tissue data sources and is provided in the next few subsections (i-ix).

i) Layer II/III pyramidal cells (FRB and RS) make isotropic connections to several of the cortical layers out to 250 μm . These connections are guided closely by the macrocolumnar connectivity provided by Traub et al. (7). There is sparse connectivity between the Layer II/III pyramidal cell system and the Layer VI pyramidal cell system, Table 4.

ii) Basket cells make connection out to a radius of 1000 μm (with isotropic probability of connections out to 250 μm then the probability decreases exponentially with the size scale of 300 μm out to 1000 μm). Supragranular basket cells connect to supragranular targets, and infragranular basket cells connect to infragranular targets. Connection numbers are illustrated in Table 4.

iii) Connections for Layer IV stellate cells are illustrated in Table 4. They are configured as RS cells (23), with firing properties guided by Traub et al. (7).

iv) Layer V pyramidal cells (RS and IB) make isotropic connections to several of the cortical layers out to 250 μm . Connection numbers are illustrated in Table 4.

v) Layer VI pyramidal cells (RS) make isotropic connections out to 250 μm as well, Table 4 & 5.

vi) Axo-axonic (chandelier) cells are a type of inhibitory cell which innervates specifically the outgoing axonal initial segments of neighboring neurons. This acts to raise the threshold on the amount of synaptic current required to generate an action potential (12). Their axonal arbors are 300-400 μm in diameter (250 μm in the model) (24), with isotropic connections demonstrated in Table 4 & 5. These cells are represented as fast spiking inhibitory cells (7).

vii) Low-threshold spiking (LTS) interneurons consist of both deep and superficial versions as in the case of basket cells. The firing behavior of these cells is characterized by an initial burst generated by low-threshold calcium channels (7,9,25). Isotropic connections to 250 μm are demonstrated in Table 4 & 5.

viii) Thalamocortical relay cells (TCR) are represented as having 10 major branching dendritic elements. The cells are able to represent the low-threshold calcium current driven bursting behavior observed in vivo with microelectrode recordings (7,26). The TCR connectivity to the cortical component is demonstrated in Table 4.

ix) Nucleus reticular thalami inhibitory cells (nRT) are introduced with a similar architecture as the other inhibitory cells in the model (7), the subcortical connectivity is described in Table 4.

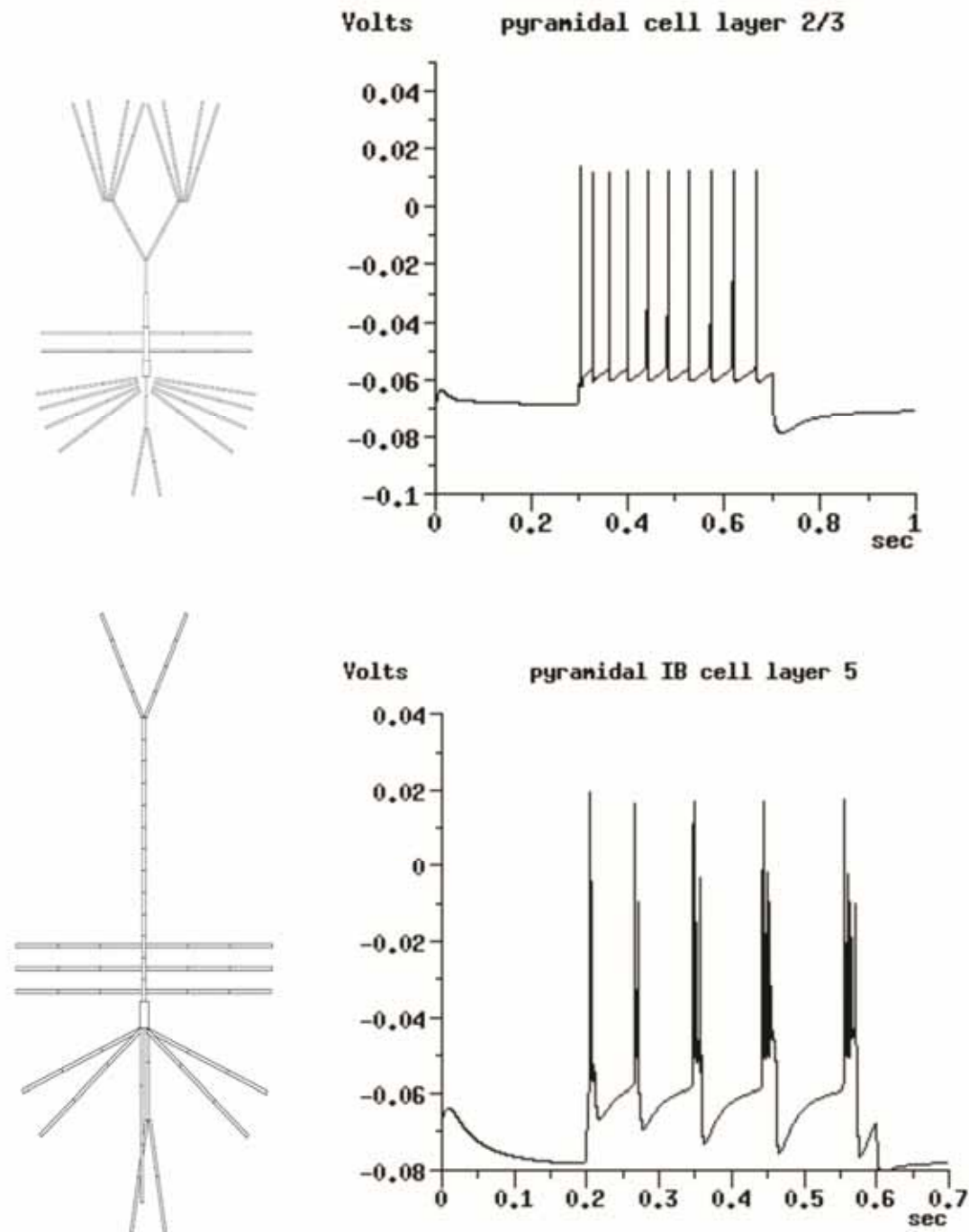


Figure 1A Modeled pyramidal cells in layer II/III (upper panel) and the intrinsically bursting pyramidal cell in layer 5 (bottom). Numbers of compartments in the cell renderings are 74 and 61 respectively. Current injections: 0.75 nA and 1.3 nA.

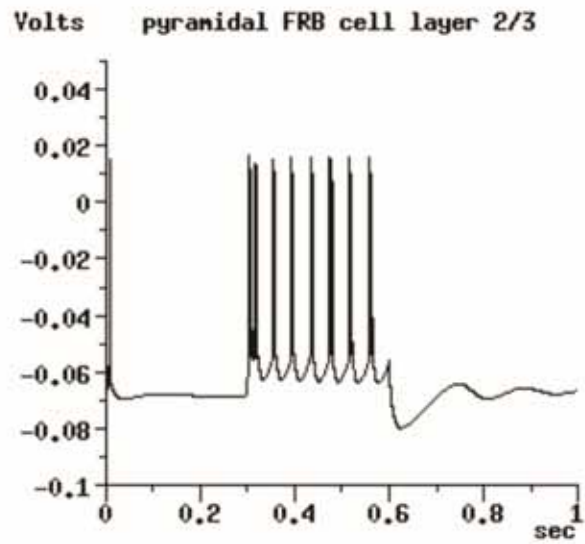
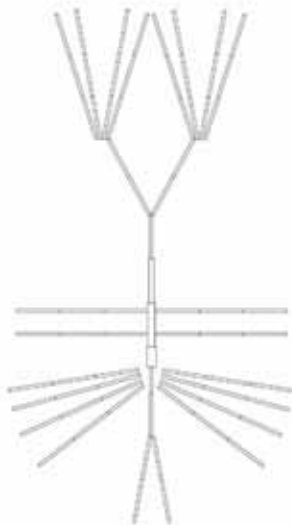
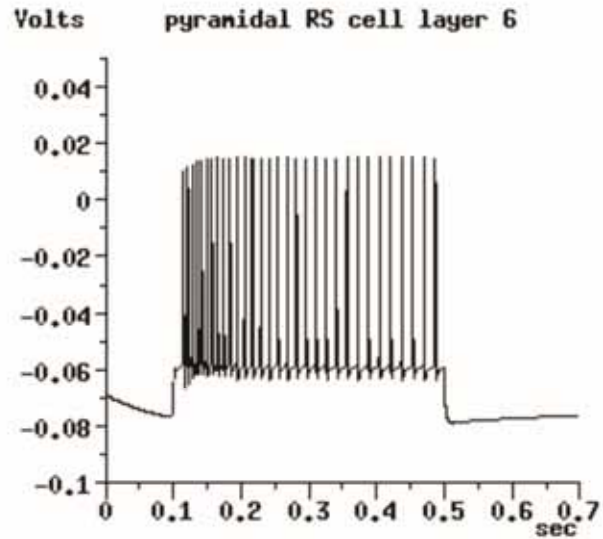
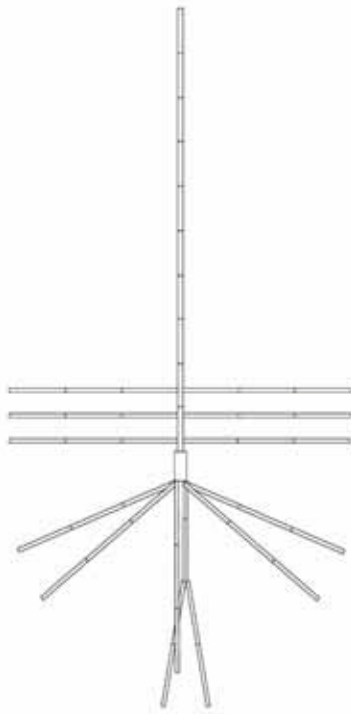


Figure 1B The modeled pyramidal cell in layer VI (upper panel) and the fast rhythmic bursting pyramidal cell in layer II/III (bottom). Numbers of compartments are 50 and 74 respectively. Current injections: 0.1 nA and 0.4 nA.

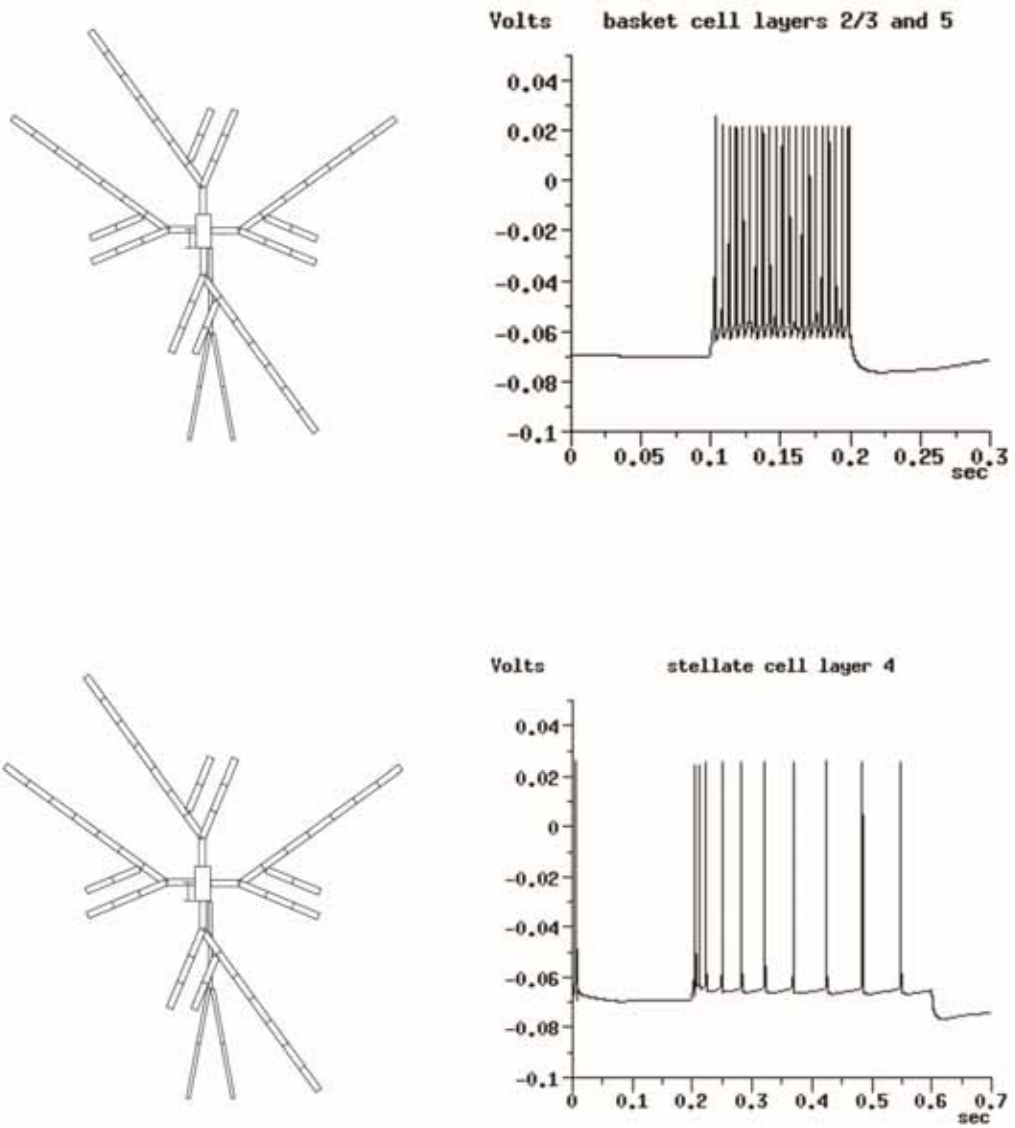


Figure 1C The model for basket cells in layers II/III & V (upper panel) and the stellate cell in layer IV (bottom). The number of compartments in both cell models is 59. Current injections: 0.4 nA and 0.3 nA.

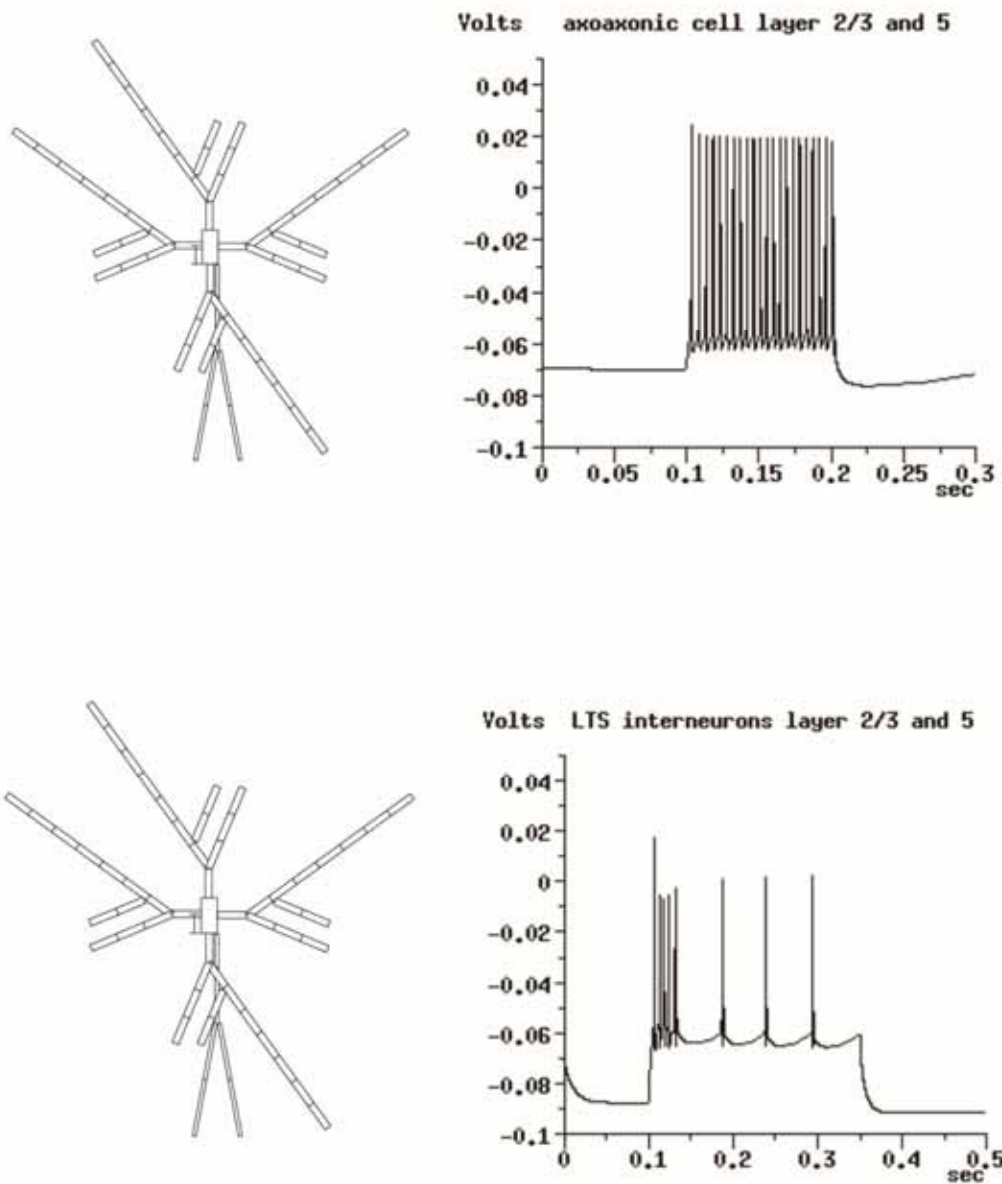


Figure 1D The model rendering of axo-axonic cells in layers II/III & V (upper panel) and the low threshold spiking cells in layers II/III & V (bottom). The number of compartments in both cell models is 59. Current injection: 0.4 nA (in both).

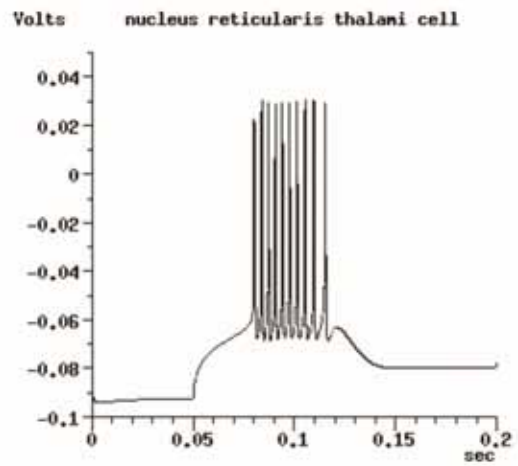
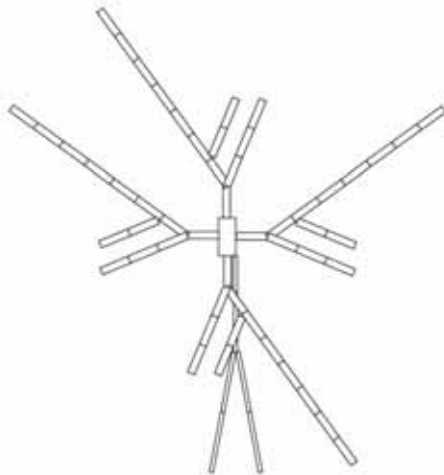
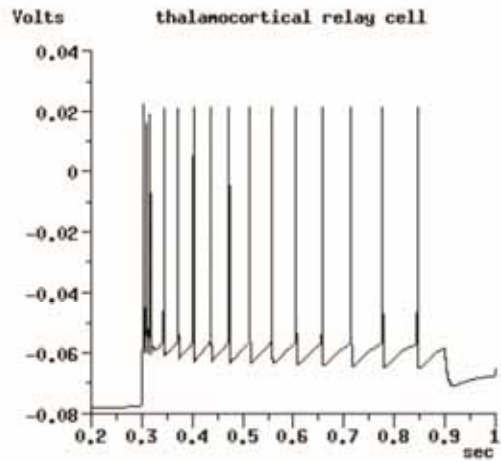
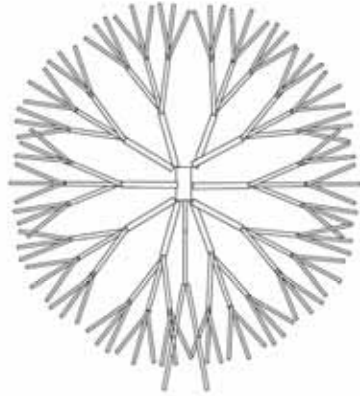


Figure 1E The model rendering of thalamocortical relay cell (upper panel) and the reticular thalamic cell (bottom). The number of compartments is 137 and 59 respectively. Current injection 0.4 nA (in both).

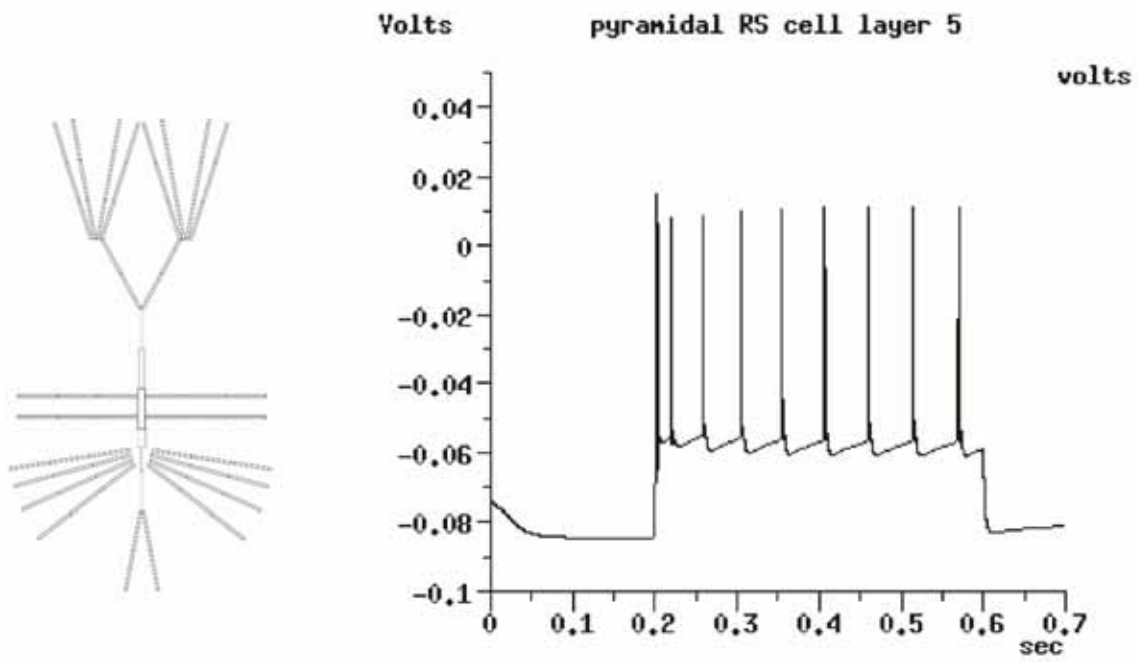


Figure 1F The model rendering of pyramidal cell in layer V. Numbers of compartments is cell model is 74. Current injections: 1.3 nA.

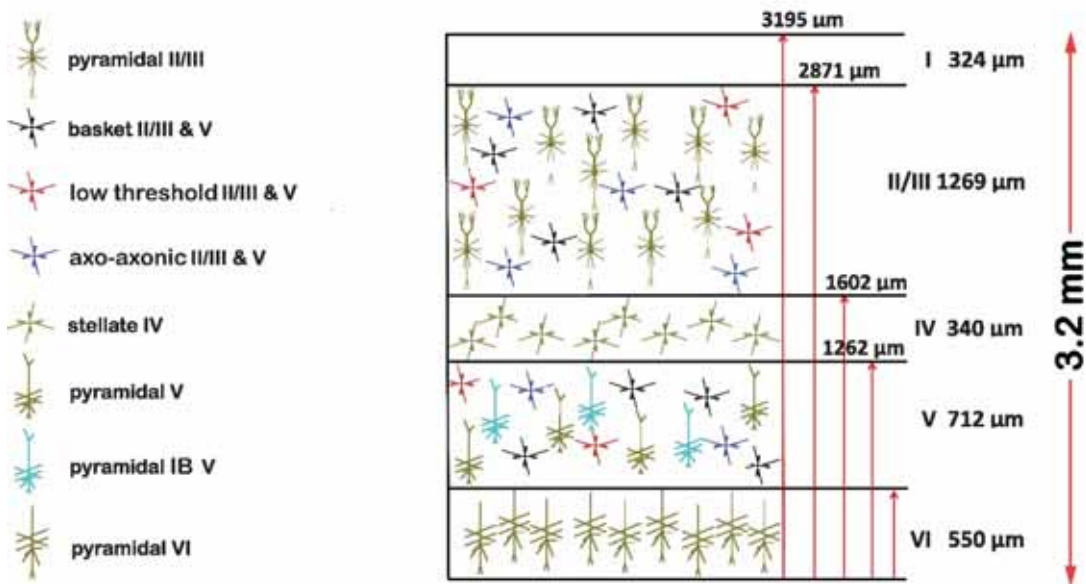


Figure 1 Distribution of compartmental models of cortical neurons in the x-z plane in the simulated cortical volume. The supragranular layer consists of basket, low-threshold, axo-axonic and pyramidal neurons in layers II/III, the internal granular layer is represented by stellate neurons in layer IV, and the infragranular layer consists of basket, low-threshold and axo-axonic neurons in layer V and pyramidal neurons in layers V and VI. The position of a neuron within a modeled volume is defined by the Cartesian coordinates $[x,y,z]$ of the soma. The vertical arrangement of neuron types into a layered structure was obtained by assigning z coordinates of neurons within a given range that is pre-determined for each cell type (with the exceptions of thalamic cells that are held at fixed position below layer VI). The z coordinate of each neuron within a given layer was randomized and each neuron is rotated about its normal axis by a random angle from 0 to 360 degrees. In horizontal directions we use an array of repeating minicolumns. The arrangement of neurons in layers and minicolumns provides a spatial scale in both vertical and horizontal directions. An array of 40x40 repeating minicolumns represents approximately 1 mm x 1 mm of cortex. The cellular density in the model varies from 630 (basket) to 5043 (pyramidal) neurons/mm³. Note: The sizes of the illustrated neurons were chosen arbitrary for better visualization. In fact the apical dendritic trunks of pyramidal neurons project to upper cortical layers. The vertical scale on the right side refers to the high of the modeled cortical layers rather than the lengths of apical, oblique and basal dendrites or inter-neuronal distances.

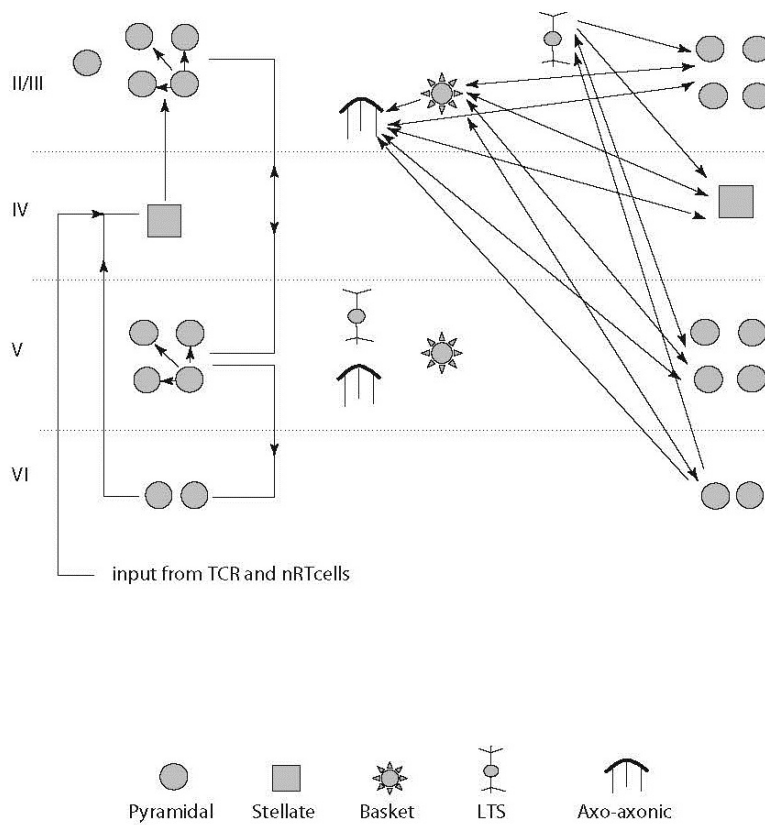


Figure 3. Schematics diagram of the types of neurons as well as their intrinsic connectivity within a minicolumn. Neurons may connect both with neurons in their minicolumn and in other minicolumns. The connection pattern relies heavily on the visual cortical model of Douglas and Martin (12). For some of the external connections left out of that model description the simulation includes connections described by Nieuwenhuys (13) in his summary of the anatomic data. Specifically, these additional external connections are from the layer II/III pyramidal cells to distant layer V pyramidal cells. The visual cortical model wiring was used for the minicolumns because it has been widely studied over a long period of time, and seems to have analogs in other regions of somatosensory cortex (12). It has also been used in previous single compartment simulations of neocortex (1,27,28).

Table 1. Membrane conductance densities (mS/cm²):

Supragranular pyramidal neurons (layer II/III)

	gNa(F)	gNa(P)	gK(DR)	gK(gK(gK(gK	gK(A	gCa	gCa	gAR
axon	400	0	400	0	2	0	0.1	0	0	0	0
soma	187.5	0.12	125	12	30		0.1	0.04	1	0.1	
distal	12.5-12.5	0.008-0.008	6.25-125	12	2-		0.1	0.04	1	0.1	0.25

Supar- and infragranular basket neurons (layer II/III & V)

	gNa(F)	gNa(P)	gK(DR)	gK(gK(gK(gK	gK(A	gCa	gCa	gAR
axon	400	0	400	0	1	0	0	0	0	0	0
soma	60	0	100	25	1	0	0	0	0.1	0	0
distal	60	0	100	25		0	0	0	0.1	0	0
	10	0	10	25		0	0	0	0.2	0	0

Internal granular stellate neurons (layer IV)

	gNa	gNa(P)	gK(gK(gK(gK(gK	gK(A	gCa	gCa	
axon	40	0.4	40	0	2	0	0.1	0	0	0	0
soma	150	0.15	10	10	30	3.75	0.1	0.1	0.5	0.1	0.25
distal	75	0.075	75	10	2-	3.75	0.1	0.1	0.5	0.1	0.25
	5	0.005	0	10	2	3.75	0.1	0.1	0.5	0.1	0.25

Infragranular pyramidal neurons (layer V)

	gNa	gNa(P)	gK(gK(gK(gK(gK	gK(A	gCa	gCa	gAR
soma	45	0	45	0	0.	30		0	0	0	0
	20	0.16	170	28.8	2	8.5		0.2	1.6	0.1	
distal	75-	0.06-0.012	0-	0.9-28.8	0.6-	13.6		0.2	0.4-	0.1	
			0	2.16		4		0.2			

Infragranular pyramidal neurons (layer VI)

	gNa	gNa(P)	gK(D	gK(g(gK(gK	gK(A	gCa	gC	
soma	45	0	450	0	4	0	0.1	0	0	0	0
	20	0.08	170	15	122.5	4.2	0.1	0.2	0.2	0.1	0.25
distal	75	0.03	75	15	13.6	4.2	0.1	0.2	0.2	0.1	0.25
	5	0.002	0	0	13.6	4.2	0.1	0.2	0.2	0.1	0.25

Table 2 AMPA and GABA_A synaptic model parameters

AMPA or GABA_A: $G_k = g_{\max} \frac{t}{\tau_1} (e^{-t/\tau_1})$ where g_{\max} [nS] and τ [ms] are provided in the table below:

	postsynaptic													
	P23RS	P23FRB	B23FS	I23LTS	C23FS	ST4RS	P5RS	P5IB	B5FS	C5FS	I5LTS	P6RS	nRT	TCR
P23RS	0.25nS 2.0ms	0.25nS 2.0ms	3.0nS 0.8ms	2.0nS 1.0ms	3.0nS 0.8ms	0.1nS 2.0ms	0.1nS 2.0ms	0.1nS 2.0ms	1.0nS 0.8ms	1.0nS 0.8ms	1.0nS 1.0ms	0.5nS 2.0ms		
P23FRB	0.25nS 2.0ms	0.25nS 2.0ms	3.0nS 0.8ms	2.0nS 1.0ms	3.0nS 0.8ms	0.1nS 2.0ms	0.1nS 2.0ms	0.1nS 2.0ms	1.0nS 0.8ms	1.0nS 0.8ms	1.0nS 1.0ms	0.5nS 2.0ms		
B23FSI	1.2nS 6.0ms	1.2nS 6.0ms	0.2nS 2.0ms	0.5nS 3.0ms	0.2nS 2.0ms	0.1nS 6.0ms								
I23LTS	0.01nS 20.0ms	0.01nS 20.0ms	0.01nS 20.0ms	0.05nS 20.0ms	0.01nS 20.0ms	0.01nS 20.0ms	0.01nS 20.0ms	0.02nS 20.0ms	0.01nS 20.0ms	0.01nS 20.0ms	0.05nS 20.0ms	0.01nS 20.0ms		
C23FS	1.2nS 6.0ms				1.2nS 6.0ms	0.1nS 6.0ms	1.0nS 6.0ms	1.0nS 6.0ms				1.0nS 6.0ms		
ST4RS	1.0nS 2.0ms	1.0nS 2.0ms	1.0nS 0.8ms	1.0nS 0.8ms		1.0nS 2.0ms	1.0nS 2.0ms	1.0nS 2.0ms	1.0nS 0.8ms		1.0nS 0.8ms	1.0nS 2.0ms		
P5RS	0.5nS 2.0ms	1.0nS 0.8ms	1.0nS 0.8ms	1.0nS 1.0ms	1.0nS 0.8ms	0.5nS 2.0ms	2.0nS 2.0ms	2.0nS 2.0ms	3.0nS 0.8ms	2.0nS 0.8ms	2.0nS 1.0ms	2.0nS 2.0ms		
P5IB	0.5nS 2.0ms	0.5nS 2.0ms	1.0nS 0.8ms	1.0nS 1.0ms	1.0nS 0.8ms	0.5nS 2.0ms	2.0nS 2ms	2.0nS 2.0ms	2.0nS 0.8ms	3.0nS 0.8ms	2.0nS 1.0ms	2.0nS 2.0ms		
B5FS							0.7nS 6.0ms	0.7nS 6.0ms	0.7nS 6ms	0.2nS 3.0ms	0.7nS 3.0ms			
C5FS	1.0nS 6.0ms	1.0nS 6.0ms				1.5nS 6.0ms	1.0nS 6.0ms	1.0nS 6.0ms				1.0nS 6.0ms		
I5LTS	0.01nS 20.0ms	0.01nS 20.0ms	0.01nS 20.0ms	0.05nS 20.0ms	0.01nS 20.0ms	0.01nS 20.0ms	0.02nS 20.0ms	0.05nS 20.0ms	0.01nS 20.0ms	0.01nS 20.ms	0.05nS 20.0ms	0.01nS 20.0ms		
P6RS	0.5nS 2.0ms	0.5nS 2.0ms	1.0nS 0.8ms	1.0nS 1.0ms	1.0nS 0.8ms	0.5nS 2.0ms	1.0nS 2.0ms	1.0nS 2.0ms	3.0nS 0.8ms	3.0nS 0.8ms	2.0nS 1.0ms	1.0nS 2.0ms	0.5nS 1.0ms	0.75nS 1.0ms
nRT													0.3nS 9.0ms,44.5ms	0.7- 2.1nS 6.9ms
TCR	0.50nS 2.0ms	0.5nS 2.0ms	0.1nS 1.0ms		0.1nS 1.0ms	1.0nS 2.0ms	1.5nS 2.0ms	1.5nS 2.0ms	1.5nS 1.0ms	1.5nS 1.0ms		1.0nS 2.0ms	0.75nS 2.0ms	

Legend: P23RS, P5RS supra- and infragranular pyramidal neurons (Layer II/III & V respectively)
P23FRB supragranular fast rhythmic bursting pyramidal neurons (Layer II/III)
B23FS, B5FS supar- and infragranular basket neurons (layer II/III & V respectively)
C23FS, C5FS supar- and infragranular axo-axonic neurons (layer II/III & V respectively)
I23LTS, I5LTS supar- and infragranular low threshold spiking neurons (layer II/III & V respectively)
ST4RS internal granular stellate neurons (layer IV)
P5IB infragranular intrinsically bursting pyramidal neurons (Layer V)
P6RS infragranular pyramidal neurons (Layer VI)
TCR,nRT thalamocortical relay and reticular nucleus thalamic neurons respectively

Table 2 (cont) NMDA synaptic model parameters

NMDA: $G_k = g_{\max} \frac{e^{-t/\tau_1} - e^{-t/\tau_2}}{1 + \eta [Mg^{2+}] e^{-\gamma V}}$ where $\eta = 0.33/\text{mM}$, $\gamma = 0.06/\text{mV}$ and $\tau_2 = 0.67 \text{ ms}$; g_{\max} [nS] and τ_1 [ms] are provided in the table below.

postsynaptic

presynaptic

	P23RS	P23FRB	B23FS	I23LTS	C23FS	ST4RS	P5RS	P5IB	B5FS	C5FS	I5LTS	P6RS	nRT	TCR
P23RS	0.025nS 130ms	0.025nS 130ms	0.15nS 100ms	0.15nS 100ms	0.15nS 100ms	0.01nS 130ms	0.01nS 130ms	0.01nS 130ms	0.1nS 100ms	0.1nS 100ms	0.15nS 100ms	0.05nS 130ms		
P23FRB	0.025nS 130ms	0.025nS 130ms	0.15nS 100ms	0.15nS 100ms	0.15nS 100ms	0.01nS 130ms	0.01nS 130ms	0.01nS 130ms	0.1nS 100ms	0.1nS 100ms	0.15nS 100ms	0.05nS 130ms		
ST4RS	0.1nS 130ms	0.1nS 130ms	0.15nS 100ms	0.15nS 100ms		0.1nS 100ms	0.1nS 130ms	0.1nS 100ms	0.15nS 100ms		1.0nS 0.8ms	0.1nS 130ms		
P5RS	0.05nS 130ms	0.05nS 130ms	0.15nS 100ms	0.15nS 100ms	0.15nS 100ms	0.05nS 130ms	0.2nS 130ms	0.2nS 130ms	0.15nS 100ms	0.15nS 100ms	0.15nS 100ms	0.2nS 130ms		
P5IB	0.05nS 130ms	0.05nS 130.0.67ms	0.15nS 100ms	0.15nS 100ms	0.15nS 100ms	0.05nS 130ms	0.20nS 100ms	0.20nS 130ms	0.15nS 100ms	0.15nS 100ms	0.15nS 100ms	0.2nS 130ms		
P6RS	0.05nS 130ms	0.05nS 100ms	0.1nS 100ms	0.1nS 100ms	0.1nS 100ms	0.05nS 130ms	0.1nS 130ms	0.1nS 100ms	0.1nS 100ms	0.1nS 100ms	0.1nS 100ms	0.1nS 130ms	0.05nS 100ms	0.075nS 130ms
TCR	0.05nS 130ms	0.05nS 130ms	0.01nS 100ms		0.01nS 100ms	0.1nS 130ms	0.15nS 130ms	0.15nS 130ms	0.1nS 100ms	0.1nS 100ms		0.1nS 130ms	0.15nS 150ms	

Legend: P23RS, P5RS supra- and infragranular pyramidal neurons (Layer II/III & V respectively)
P23FRB supragranular fast rhythmic bursting pyramidal neurons (Layer II/III)
B23FS, B5FS supar- and infragranular basket neurons (layer II/III & V respectively)
C23FS, C5FS supar- and infragranular axo-axonic neurons (layer II/III & V respectively)
I23LTS, I5LTS supar- and infragranular low threshold spiking neurons (layer II/III & V respectively)
ST4RS internal granular stellate neurons (layer IV)
P5IB infragranular intrinsically bursting pyramidal neurons (Layer V)
P6RS deep infragranular pyramidal neurons (Layer VI)
TCR,nRT thalamocortical relay and reticular nucleus thalamic cells respectively

Table 3 Gap junction current model parameters.

Electrical coupling (between presynaptic and postsynaptic neuronal compartments) is modeled as: $I_{gap} = g_{gap} (V_{pre} - V_{post})$.

Gap junction conductances g_{gap} [nS] and connection probabilities are provided in the table below.

		postsynaptic											
presynaptic		P23RS	P23FRB	B23FS	I23LTS	ST4RS	P5RS	P5IB	B5FS	I5LTS	P6RS	nRT	
	P23RS	2.0nS 0.0056	3.0nS 0.0234										
	P23FRB		3.0nS 0.0025										
	B23FS			1.0nS 0.069									
	I23LTS				1.0nS 0.0694								
	ST4RS					3.0nS 0.0312							
	P5RS						4.0nS 0.0547						
	P5IB						4.0nS 0.0031	4.0nS 0.0034					
	B5FS								1.0nS 0.0078				
	I5LTS									1.0nS 0.0781			
	P6RS										4.0nS 0.0156		
	nRT											1.0nS 0.0781	

- Legend:** P23RS, P5RS supra- and infragranular pyramidal neurons (Layer II/III & V respectively)
P23FRB supragranular fast rhythmic bursting pyramidal neurons (Layer II/III)
B23FS, B5FS supar- and infragranular basket neurons (layer II/III & V respectively)
I23LTS, I5LTS supar- and infragranular low threshold spiking neurons (layer II/III & V respectively)
ST4RS internal granular stellate neurons (layer IV)
P5IB infragranular intrinsically bursting pyramidal neurons (Layer V)
P6RS deep infragranular pyramidal neurons (Layer VI)
nRT reticular nucleus thalamic neurons

Table 4 Numbers of neurons (presynaptic) contacting a given postsynaptic neuron and the corresponding probabilities of connections:

		postsynaptic														
presynaptic		P23RS	P23FRB	B23FS	I23LTS	C23FS	ST4RS	P5RS	P5IB	B5FS	C5FS	I5LTS	P6RS	nRT	TCR	
	P23RS	26 (0.003)	26 (0.003)	48 (0.008)	48 (0.008)	48 (0.008)	1 (0.0025)	32 (0.015)	32 (0.015)	16 (0.003)	16 (0.0026)	16 (0.0026)	1 (0.00075)			
	P23FRB	3 (0.0055)	3 (0.006)	3 (0.008)	3 (0.008)	3 (0.008)	0 (0.0017)	2 (0.0015)	1 (0.008)	1 (0.005)	2 (0.005)	2 (0.005)	0 (0.005)			
	B23FS	10 (0.03)	10 (0.03)	10 (0.015)	10 (0.014)	10 (0.014)	10 (0.066)									
	I23LTS	10 (0.0063)	10 (0.0063)	10 (0.008)	10 (0.0085)	10 (0.008)	10 (0.008)	10 (0.008)	10 (0.008)	10 (0.014)	10 (0.014)	10 (0.014)	10 (0.011)			
	C23FS	10 (0.333)	10 (0.333)				2 (0.083)	2 (0.083)	2 (0.083)				2 (0.083)			
	ST4RS	10 (0.007)	10 (0.007)	10 (0.007)	10 (0.007)	10 (0.007)	16 (0.01)	10 (0.014)	10 (0.014)	10 (0.007)	10 (0.007)	10 (0.007)	10 (0.033)			
	P5RS	1 (0.001)	1 (0.0012)	10 (0.07)	10 (0.07)	10 (0.07)	10 (0.07)	5 (0.018)	10 (0.0036)	10 (0.007)	10 (0.007)	10 (0.007)	10 (0.004)			
	P5IB	1 (0.0003)	1 (0.0003)	10 (0.0017)	10 (0.0017)	10 (0.0017)	10 (0.0017)	10 (0.0009)	25 (0.0022)	10 (0.0017)	10 (0.0017)	10 (0.0017)	10 (0.0009)			
	B5FS						10 (0.07)	10 (0.042)	10 (0.042)	10 (0.014)	10 (0.014)	10 (0.014)	10 (0.048)			
	C5FS	2 (0.333)	3 (0.333)				3 (0.083)	3 (0.083)	2 (0.083)				2 (0.083)			
	I5LTS	5 (0.0063)	5 (0.0063)	5 (0.0083)	5 (0.0085)	5 (0.0083)	10 (0.0082)	10 (0.0083)	10 (0.0083)	10 (0.014)	10 (0.014)	10 (0.014)	10 (0.011)			
	P6RS	5 (0.01)	5 (0.01)	5 (0.0017)	5 (0.0017)	5 (0.0017)	5 (0.0017)	5 (0.0009)	5 (0.0009)	5 (0.0017)	5 (0.002)	5 (0.0017)	10 (0.002)	10 (0.007)	10 (0.0009)	
	nRT													5 (0.0035)	16 (0.0055)	
	TCR	5 (0.007)	10 (0.007)	5 (0.014)		5 (0.014)	8 (0.0064)	5 (0.018)	5 (0.018)	11 (0.028)	5 (0.014)		5 (0.033)	10 (0.028)		

Legend: P23RS, P5RS supra- and infragranular pyramidal neurons (Layer II/III & V respectively)
P23FRB supragranular fast rhythmic bursting pyramidal neurons (Layer II/III)
B23FS, B5FS supar- and infragranular basket neurons (layer II/III & V respectively)
C23FS, C5FS supar- and infragranular axo-axonic neurons (layer II/III & V respectively)
I23LTS, I5LTS supar- and infragranular low threshold spiking neurons (layer II/III & V respectively)
ST4RS internal granular stellate neurons (layer IV)
P5IB infragranular intrinsically bursting pyramidal neurons (Layer V)
P6RS infragranular pyramidal neurons (Layer VI)
TCR,nRT thalamocortical relay and reticular nucleus thalamic neurons respectively

Table 5. Maximum radial distances of synaptic contact areas.

	Post-Layer II/III Pyramidal Neurons	Post-Layer IV Stellate Interneurons	Post-Layer V Pyramidal Neurons	Post-Layer VI Pyramidal Neurons	Post-Basket Cells	Post-Low Threshold Spiking Interneurons	Post-Axo-Axonic Neurons
Pre-Layer II/III Pyramidal Neurons	300 μm	300 μm	300 μm		300 μm		300 μm
Pre-Layer IV Stellate Neurons	<25 μm				<25 μm		<25 μm
Pre-Layer V Pyramidal Neurons	300 μm		300 μm	<25 μm	300 μm	300 μm	300 μm
Pre-Layer VI Pyramidal Neurons	300 μm	<25 μm		<25 μm	300 μm	300 μm	300 μm
Pre-Basket Interneurons	250 μm flat, then exp decay to 1000 μm	250 μm flat, then exp decay to 1000 μm	250 μm flat, then exp decay to 1000 μm	250 μm flat, then exp decay to 1000 μm	250 μm flat, then exp decay to 1000 μm	250 μm flat, then exp decay to 1000 μm	250 μm flat, then exp decay to 1000 μm
Pre-Low Threshold Spiking Interneurons	100 μm	100 μm	100 μm		100 μm		100 μm
Pre-Axo-Axonic Cell Neurons	200 μm	200 μm	200 μm				

References

1. Anderson WS, Kudela P, Cho J, Bergey GK, Franaszczuk PJ. Studies of stimulus parameters for seizure disruption using neural network simulations. *Biol Cybern.* 2007;97(2):173–194.
2. Mai JK, Paxinos G, Voss T. Atlas of the human brain. 3rd Ed. Elsevier, New York, 2008: p. 171, Plate 39, 22.6 mm coronal slice.
3. Buxhoeveden DP, Casanova MF. The minicolumn hypothesis in neuroscience. *Brain* 2002;125: 935-951.
4. Jones EG. Microcolumns in the cerebral cortex. *Proc Natl Acad Sci.* 2000;97(10):5019-5021.
5. Köhling R, Qü M, Zilles K, Speckmann E-J. Current-source-density profiles associated with sharp waves in human epileptic neocortical tissue. *Neurosci* 1999;**94**:1039-1050.
6. Gittins R, Harrison PJ. A quantitative morphometric study of the human anterior cingulate cortex. *Brain Res* 2004;**1013**:212-222.
7. Traub RD, Contreras D, Cunningham MO, Murray H, LeBeau FE, Roopun A, Bibbig A, Wilent WB, Higley MJ, Whittington MA. Single-column thalamocortical network model exhibiting gamma oscillations, sleep spindles, and epileptogenic bursts. *J Neurophys* 2005;**93**:2194-2232.
8. Traub RD, Buhl EH, Gloveli T, Whittington MA. Fast rhythmic bursting can be induced in layer 2/3 cortical neurons by enhancing persistent Na⁺ conductance or by blocking BK channels. *J Neurophysiol* 2003;**89**:909-921.
9. Cunningham MO, Whittington MA, Bibbig A, Roopun A, LeBeau FEN, Vogt A, Monyer H, Buhl EH, Traub RD. A role for fast rhythmic bursting neurons in cortical gamma oscillations *in vitro*. *PNAS* 2004;**101**:7152-7157.
10. Bower JM, Beeman D. The book of GENESIS: exploring realistic neural models with the GEneral NEural SIMulation System. Springer, New York, 1997.
11. Bower JM, Beeman D. Constructing realistic neural simulations with GENESIS. *Meth Mol Biol* 2007;**401**:103-125.
12. Douglas RJ, Martin KAC. Neuronal circuits of the neocortex. *Ann Rev Neurosci* 2004;**27**:419-451.
13. Nieuwenhuys R. The neocortex: An overview of its evolutionary development, structural organization and synaptology. *Anat Embryol* 1994;**190**:307-337
14. Peters A, Sethares C. Myelinated axons and the pyramidal cell modules in monkey primary visual cortex. *J Comp Neurol* 1996;**365**(2):232-255.
15. Budd JM, Kisvárdy ZF. Local lateral connectivity of inhibitory clutch cells in layer 4 of cat visual cortex (area 17). *Exp Brain Res* 2001;**140**:245-250.
16. Kisvárdy ZF, Ferecsko AS, Kovacs K, Buzas P, Budd JM, Eysel UT. One axon-multiple functions: specificity of lateral inhibitory connections by large cells. *Neurocytology* 2002;**31**:255-264.
17. Lund JS, Wu CQ. Local circuit neurons of macaque monkey striate cortex: IV. Neurons of laminae 1-3A. *J Comp Neurol* 1997;**384**:109-126.
18. Defelipe J, Gonzalez-Albo MC, Del Rio MR, Elston GN. Distribution and patterns of connectivity of interneurons containing calbindin, calretinin, and parvalbumin in visual areas of the occipital and temporal lobes of the macaque monkey. *J Comp Neurol* 1999;**412**:515-526.

19. Morrow BA, Elsworth JD, Roth RH. Prenatal exposure to cocaine selectively disrupts the development of parvalbumin containing local circuit neurons in the medial prefrontal cortex of the rat. *Synapse* 2005;**56**:1-11.
20. Thomson AM, Deuchars J. Synaptic interactions in neocortical local circuits: dual intracellular recordings in vitro. *Cereb Cortex* 1997;**7**:510-522.
21. Kisvárdy ZF, Martin KA, Freund TF, Maglóczy Z, Whitteridge D, Somogyi P. Synaptic targets of HRP-filled layer III pyramidal cells in the cat striate cortex. *Exp Brain Res* 1986;**64**:541-552.
22. Krimer LS, Goldman-Rakic PS. Prefrontal microcircuits: membrane properties and excitatory input of local, medium, and wide arbor interneurons. *J Neurosci* 2001;**21**:3788-3796.
23. Melchitzky DS, Gonzalez-Burgos G, Barrionuevo G, Lewis DA. Synaptic targets of the intrinsic axon collaterals of supragranular pyramidal neurons in monkey prefrontal cortex. *J Comp Neurol* 2001;**430**(2):209-221.
24. Kawaguchi Y, Kubota Y. Neurochemical features and synaptic connections of large physiologically-identified GABAergic cells in the rat frontal cortex. *Neurosci* 1998;**85**(3):677-701.
25. Kawaguchi Y. Physiological subgroups of nonpyramidal cells with specific morphological characteristics in layer II/III of rat frontal cortex. *J Neurosci* 1995;**15**:2638-2655.
26. Steriade M, Jones EG, McCormick DA. *Thalamus*. Elsevier, Amsterdam, 1997.
27. Anderson WS, Kudela P, Weinberg S, Bergey GK, Franaszczuk PJ. Phase dependent stimulation effects on bursting activity in a neural network cortical simulation. *Epi Res* 2009;**84**:42-55.
28. Anderson WS, Azhar F, Kudela P, Bergey GK, Franaszczuk PJ. Epileptic seizures from abnormal networks: Why some seizures defy predictability. *Epi Res* 2012;**99**(3):202-213.